IIETA International Information and Engineering Technology Association
Advancing the World of Information and Engineering

Journal Européen des Systèmes Automatisés
Vol. 59, No. 3, March, 2026, pp. 707-716
Journal homepage: http://iieta.org/journals/jesa

Thermal Prediction Using Artificial Neural Networks in Electric Scooter Batteries with Phase Change Materials

Safarudin Gazali Herawan*, Ismail Azizi Martalogawa, Azqy Nur Farenzy Saputra, Ahmad Hanif

Industrial Engineering Department, Faculty of Engineering, Bina Nusantara University, Jakarta 11480, Indonesia

Corresponding Author Email: safarudin.gazali@binus.edu

https://doi.org/10.18280/jesa.590314

Received: 27 January 2026
Revised: 18 March 2026
Accepted: 26 March 2026
Available online: 31 March 2026

Keywords:
electric scooters, lithium-ion battery thermal management, beeswax phase change material, *Artificial Neural Network temperature prediction, passive battery cooling*

ABSTRACT

The rapid expansion of electric scooters in urban transportation intensifies the need for compact and efficient battery thermal management systems to ensure the safety, reliability, and longevity of lithium-ion batteries under dynamic operating conditions. Temperature fluctuations during acceleration and varying load profiles can accelerate battery degradation and reduce performance, making passive cooling strategies such as phase change materials (PCMs) increasingly attractive. This study experimentally evaluates the thermal performance of air-cooled, paraffin-based phase change material (PCM), and beeswax-based PCM battery configurations under controlled dynamic loading conditions. Thermal and electrical parameters, including temperature evolution, voltage stability, and capacity retention, were systematically recorded and compared. Results indicate that the beeswax-based PCM provides superior thermal regulation by reducing peak temperatures and improving voltage stability compared to both paraffin PCM and air cooling. To enhance predictive capability, an Artificial Neural Network (ANN) model was developed using experimental data to forecast battery temperature based on operating variables and cooling configuration. The model demonstrated strong agreement with experimental observations, confirming its ability to capture non-linear thermal behaviour. The integration of bio-based PCM with data-driven thermal prediction offers a scalable and sustainable approach for intelligent battery thermal management in micromobility applications.

1. INTRODUCTION

Electric scooters (e-scooters) have rapidly become a prominent solution for urban micromobility due to their compact design, energy efficiency, and reduced environmental impact. At the core of these vehicles lies the lithium-ion battery system, whose safety, reliability, and lifespan are strongly influenced by operating temperature. Elevated battery temperatures can accelerate capacity fade, increase internal resistance, and potentially trigger thermal runaway, making effective thermal management an essential requirement for micromobility applications [1-3]. These challenges are further intensified by fluctuating ambient temperatures and highly dynamic load profiles typical of electric scooter operation.

1.1 Recent progress in phase change material materials for battery thermal management

Recent research on lithium-ion battery thermal management has increasingly emphasized passive cooling strategies using phase change materials (PCMs). Talluri et al. [4] demonstrated that phase change material (PCM) integration can significantly reduce peak battery temperature under extreme conditions through latent heat absorption. Similarly, Madani et al. [5] numerically showed that PCM-based systems delay temperature rise during discharge cycles. More broadly, multiple numerical and experimental investigations conducted between 2020 and 2025 confirm that PCM-assisted systems can maintain battery temperature within safe operating ranges under high energy density and intermittent load conditions [6-12].

Paraffin-based PCMs remain widely adopted due to their chemical stability and suitable melting temperature range. Zhao et al. [13] analysed expanded graphite–paraffin composites and highlighted conductivity limitations of pure paraffin. Liu et al. [14] further investigated graphite-fin composite PCM systems and reported improved heat transfer performance. However, the inherently low thermal conductivity of paraffin restricts heat dissipation efficiency, particularly under rapid charge–discharge cycles, as also discussed in studies [14, 15]. To overcome this limitation, composite PCMs incorporating graphite, copper foam, carbon nanotubes, and porous matrices have been proposed to enhance thermal conductivity and structural integrity [16-19].

In parallel, bio-based PCMs such as beeswax have emerged as sustainable alternatives to petroleum-derived paraffins. Herawan et al. [3] experimentally compared paraffin and beeswax for battery cooling and observed improved thermal buffering under dynamic load conditions with beeswax. Alam et al. [20] enhanced beeswax using copper foam and demonstrated improved effective thermal conductivity. Overall, recent material innovations and PCM developments

are comprehensively documented in studies [4-6].

1.2 Integration challenges in compact battery thermal management systems

Despite the promising properties of PCMs, their integration into compact electric vehicle battery packs presents significant challenges. Wang and Leong [21] showed that battery orientation and limited spatial configuration influence PCM cooling effectiveness. Bashirpour-Bonab [22] and Pradeep and Venugopal [23] highlighted how melting–solidification characteristics affect thermal response in confined battery modules.

Under dynamic load conditions, non-uniform melting and solidification behaviour may result in uneven temperature gradients within battery packs, as reported by Bandela and Shaik [16] and Azzini [24]. Moreover, paraffin-based PCMs have shown reduced responsiveness at high discharge rates, increasing localized overheating risks in tightly packed configurations [16, 21].

Hybrid cooling solutions combining PCM with liquid cooling or fin structures have been explored to improve heat dissipation. Zeng et al. [25] optimized composite PCM–liquid cooling systems and demonstrated improved thermal performance. Xiao et al. [26] integrated fin structures to enhance heat conduction pathways, while Jilte et al. [27] proposed liquid channels within PCM modules. However, these hybrid systems increase structural complexity and may not be suitable for lightweight micromobility platforms.

Another integration challenge involves mechanical stability and reliable thermal contact. Karimi et al. [28] emphasized the importance of coupling electro-thermal modelling with physical validation. Thakur and Kumar [29] showed that numerical improvements must be verified under standardized driving cycles. Additional modelling and validation studies further underline the need for experimentally validated PCM frameworks for real-world applications [30, 31].

1.3 Bridging phase change material-based systems with Artificial Neural Network and predictive thermal management

Alongside material innovation, predictive modelling approaches have gained attention for improving battery thermal control. Wang et al. [32] reviewed deep neural network approaches for lithium-ion battery state prediction and highlighted their capability in modelling nonlinear electro-thermal behaviour. Chen et al. [33] applied neural network regression to hybrid battery thermal management systems and demonstrated strong temperature prediction performance under fast charging conditions.

Artificial Neural Networks (ANNs) are particularly effective in capturing non-linear relationships between operational parameters and battery temperature [32-34]. Beyond temperature prediction, ANN-based frameworks have been applied to estimate the state of health, heat generation rate, and remaining useful life of lithium-ion batteries [35-39]. For example, Gao et al. [36] developed a hybrid deep learning model for battery life prediction, while Cao et al. [39] compared machine learning algorithms and confirmed the superiority of neural networks in capturing thermal nonlinearity.

Although ANN applications in battery systems are expanding, many studies rely heavily on simulated datasets or hybrid numerical frameworks. Experimentally validated ANN–PCM integration frameworks, particularly for compact electric scooter platforms operating under dynamic load conditions, remain limited.

Consequently, there remains a research gap in combining sustainable PCM materials with experimentally trained ANN models for real-time temperature prediction in micromobility battery systems. Addressing this gap is critical for developing intelligent, scalable, and energy-efficient thermal management strategies for electric scooters.

2. METHOD

2.1 Experimental rig design and validation

A custom experimental rig was developed to replicate the mechanical and thermal conditions experienced by electric scooter battery systems. The rig employed a 1500 W brushless direct current (BLDC) motor controlled by a SiAECOSYS VOTOL motor controller (50 A), enabling precise regulation of rotational speed and torque. Mechanical load was applied through an adjustable braking mechanism to simulate incremental riding conditions.

The battery pack consisted of 78 lithium-ion cells arranged in a 13-series configuration, delivering a nominal voltage of 48 V. A Jikong battery management system (BMS) was integrated to monitor individual cell voltages and battery temperature in real time. Voltage, current, temperature, and motor speed data were recorded at one-minute intervals using a synchronized data acquisition system. The specifications of the components are listed in Table 1.

Table 1. The components specifications

No.	Component	Specification
1	BLDC Motor	1500 W
2	SiAECOSYS VOTOL Controller	50 A
3	Battery pack with 13 series of 6 batteries. Total 78 batteries	48 V 15 A
4	Throttle	Potentiometer with spring
5	Display	RPM / Speed and Battery capacity
6	Jikong BMS	Voltage sensor for 13 series battery and battery temperature

During the discharge cycle, current was not left uncontrolled. The discharge current was regulated indirectly through the motor controller by adjusting throttle input and mechanical braking load. The SiAECOSYS VOTOL controller limited the maximum current to 50 A, ensuring consistent and repeatable load increments. At each 3-minute load stage (0%, 25%, 50%, 75%, and 100%), the controller maintained stable current draw within ± 3% variation. Real-time current measurements were recorded via the BMS logging system to verify load consistency across repeated experiments.

Prior to thermal testing, structural integrity of the rig was validated using finite element analysis. Maximum equivalent stress and displacement values were found to be well below material limits, ensuring mechanical stability and minimizing experimental error during testing.

2.1.1 Temperature measurement and data acquisition

Battery temperature measurements were obtained using the built-in temperature sensor integrated within the Jikong BMS. The BMS is equipped with an internal NTC thermistor sensor directly attached to the battery pack and designed for real-time thermal monitoring during operation. Temperature data were transmitted via Bluetooth and displayed on the BMS dashboard interface accessed through a laptop and smartphone application.

The BMS provides continuous monitoring of battery voltage, current, and temperature at the pack level. Temperature readings were recorded at one-minute intervals simultaneously with voltage, current, RPM, and load data to ensure synchronized dataset acquisition for both experimental analysis and ANN modelling.

Prior to experimentation, the BMS temperature sensor readings were verified against a calibrated external digital thermometer at room temperature conditions (approximately 25 ℃). The observed deviation was within ± 0.5 ℃, which is within the manufacturer's specified tolerance range. Because the study focuses on comparative thermal behavior between cooling configurations under identical experimental conditions, this level of measurement accuracy was considered acceptable.

It should be noted that temperature measurements represent pack-level temperature rather than individual cell hotspot distribution. However, since all cooling configurations were tested under identical load profiles and environmental conditions, the comparative thermal trends remain valid and consistent for performance evaluation.

2.2 Phase change material configuration and encapsulation method

The PCM materials (paraffin wax and beeswax) were applied in a fully encapsulated configuration surrounding the battery pack. Prior to application, both PCM materials were melted separately at controlled temperatures (approximately 70–80 ℃ for paraffin and 62–65 ℃ for beeswax) to ensure uniform liquid consistency. The molten PCM was then poured into a custom-fabricated acrylic enclosure containing the assembled battery pack, allowing the material to fill the void spaces and form a continuous thermal interface layer around the cells.

The lithium-ion cells (18650 type, 65 mm height) were arranged in a single-layer configuration with an inter-cell spacing of approximately 2 mm. This spacing allowed the molten PCM to fully penetrate and surround each individual cylindrical cell, ensuring direct thermal contact between the PCM and the lateral surface of every cell.

During the casting process, the PCM was poured into the enclosure until it reached a vertical height of approximately 55 mm, measured from the base of the cell. Since the total cell height is 65 mm, the upper and lower terminal regions (approximately 5 mm at the top and 5 mm at the bottom) were intentionally left unfilled. This design prevented direct contact between the PCM and the electrical interconnections, including the cell tabs and series welding joints, thereby avoiding potential electrical insulation interference or mechanical stress during phase transition.

Consequently, the PCM encapsulated the entire lateral cylindrical surface of each cell while leaving the electrical connection zones exposed. This configuration ensured effective radial heat absorption from the cell body while maintaining electrical safety and structural integrity of the battery assembly.

The PCM was not micro-encapsulated; instead, it was macro-encapsulated within the rigid acrylic casing to prevent leakage during phase transition. This enclosure ensured structural stability during repeated melting–solidification cycles while maintaining consistent geometric configuration across all experimental runs.

All three configurations (air-cooled, paraffin PCM, beeswax PCM) used identical enclosure dimensions to ensure that any thermal performance differences resulted from material properties rather than structural variations. Figure 1 shows the battery pack configurations of no PCM, paraffin PCM, and beeswax PCM.

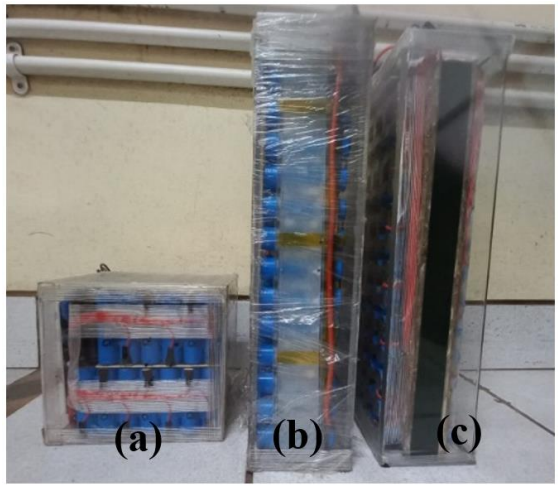

Figure 1. Battery pack configurations: (a) no phase change material (PCM), (b) paraffin PCM, (c) beeswax PCM

The testing protocol consisted of a 15-minute discharge cycle, during which mechanical load was increased stepwise from 0% to 100% in 25% increments every three minutes. This procedure was designed to emulate realistic acceleration and load variations experienced by electric scooters. Battery temperature, voltage, and capacity data were continuously monitored throughout the test.

Each battery configuration underwent identical load cycles to facilitate direct comparison. Voltage, temperature, and battery capacity were recorded at one-minute intervals. Figure 2 illustrates the rig setup used for this purpose, while Figure 3 displays the distinct physical configurations of the battery packs: air-cooled, paraffin-cooled, and beeswax-cooled.

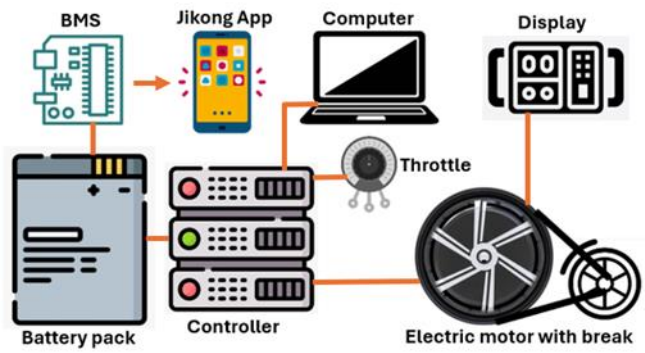

Figure 2. Schematic diagram of the experimental setup for battery thermal testing

Figure 3. Experimental rig

2.3 Artificial Neural Network Model Development

Complementing the experimental efforts, an Artificial Neural Network (ANN) model was developed to predict battery temperature as a function of real-time operating conditions and PCM integration. The model was trained using the empirical dataset obtained from the experimental tests. Its objective was to simulate battery thermal response under different PCM configurations and load levels, enabling predictive insights into battery performance and potential overheating scenarios.

The model input variables included rotational speed (RPM), mechanical load level (%), PCM type (encoded categorically), and voltage ratio. The voltage ratio is defined as the normalized battery voltage expressed as:

$$Voltage\ ratio = \frac{V_{final}}{V_{initial}} \quad (1)$$

where, V_{final} is the instantaneous measured pack voltage during discharge and $V_{initial}$ is the initial voltage at the beginning of the cycle. This normalization was applied to eliminate scale dependency and improve ANN convergence stability. These variables were selected for their known influence on battery temperature and for their availability from the experimental dataset.

The output variable was defined as the temperature ratio rather than the absolute battery temperature in degrees Celsius. The temperature ratio is expressed as the normalized value between the final measured temperature and the initial temperature at the beginning of the discharge cycle:

$$Temperature\ ratio = \frac{T_{final}}{T_{initial}} \quad (2)$$

This normalization was applied because each battery pack exhibited slightly different initial temperature conditions prior to testing. Relying solely on final temperature values could therefore introduce bias in comparative analysis. By using a temperature ratio, the model captures the relative thermal rise during operation, enabling fair comparison across configurations and improving consistency in ANN training.

The ANN architecture employed a feedforward multilayer perceptron (MLP) with a 4-4-1 structure: four input neurons, four hidden neurons, and a single output neuron. The hidden layer used the hyperbolic tangent (Tanh) activation function, while the output layer utilized a linear activation function to predict continuous temperature values. This configuration was selected based on findings from studies [32, 34], who demonstrated the effectiveness of Tanh activations in modelling non-linear thermal relationships.

The ANN model was trained using supervised learning with backpropagation optimization. The loss function was the Mean Squared Error (MSE), with model performance evaluated via standard metrics: MSE, Root Mean Squared Error (RMSE), Mean Absolute Error (MAE), and R-squared (R^2).

Integrating the ANN model with the experimental testing approach provides a robust framework for evaluating and predicting battery thermal behaviour. Not only does this dual approach validate the superiority of PCM for heat management, but it also offers a scalable method for real-time thermal forecasting in practical battery management systems. Such hybrid methodologies are increasingly advocated in literature for advancing predictive control in energy systems [36, 37].

This study's methodology incorporates a structured experimental design and data-driven modelling approach to evaluate the effectiveness of bio-based PCM materials in thermal management. The combination of a validated experimental rig and an ANN prediction model ensures that the results are both empirically grounded and computationally scalable for broader applications in micromobility energy systems.

2.4 Artificial Neural Network dataset preparation and training procedure

Although the discharge experiment lasted 15 minutes per configuration, the dataset was not limited to 15 samples. Temperature, voltage, RPM, and load were recorded at one-minute intervals across three cooling configurations and five load stages, producing multiple structured samples for ANN training. Nevertheless, the dataset remains moderate in size; therefore, additional measures were implemented to mitigate overfitting risk.

To enhance model robustness, k-fold cross-validation (k = 5) was applied during training. In this approach, the dataset was divided into five subsets, and the model was trained iteratively using four subsets for training and one subset for validation. The final performance metrics were averaged across folds. This procedure reduces variance bias and provides a more reliable estimate of generalization performance.

No artificial data augmentation was performed, in order to preserve the physical integrity of the experimental dataset. Instead, model complexity was intentionally kept low (single hidden layer with four neurons) to avoid over-parameterization relative to dataset size. Early stopping based on validation loss convergence was also implemented to prevent overfitting.

3. RESULTS AND DISCUSSION

3.1 Thermal profile under dynamic load

The comparative thermal profiles shown in Figure 4 indicate that beeswax PCM consistently suppresses peak temperature more effectively than paraffin PCM and air cooling. Although the absolute temperature reduction appears

modest (maximum difference of 3.7 °C compared to paraffin), this margin is thermally significant in lithium-ion systems, where even small temperature elevations can accelerate degradation mechanisms and reduce cycle life [4]. Previous experimental findings also reported improved thermal buffering behavior of beeswax compared to paraffin under dynamic discharge conditions [3], supporting the trend observed in this study.

The observed performance difference can be attributed to two interacting factors: latent heat absorption characteristics and melting uniformity. Beeswax exhibits a broader melting range compared to paraffin, enabling more gradual heat absorption during stepwise load increments. This behavior reduces thermal overshoot during rapid load transitions, particularly at 75–100% load levels, consistent with prior comparative analysis of beeswax and paraffin PCM in battery cooling systems [3].

In contrast, paraffin PCM demonstrates a relatively sharper phase transition behavior, which may lead to localized thermal saturation once partial melting occurs. Such behavior has been discussed in PCM-based battery modules operating under extreme temperature conditions [4]. This phenomenon could explain the steeper temperature gradient observed after minute 9 of the discharge cycle. The air-cooled configuration lacks any latent heat buffering mechanism, resulting in continuous temperature accumulation proportional to load increase.

The heatmap in Figure 5 further supports this interpretation, illustrating smoother temporal temperature evolution in the beeswax configuration. This indicates improved thermal inertia and reduced fluctuation amplitude under dynamic loading, reinforcing the role of phase transition characteristics in stabilizing battery temperature [3, 4].

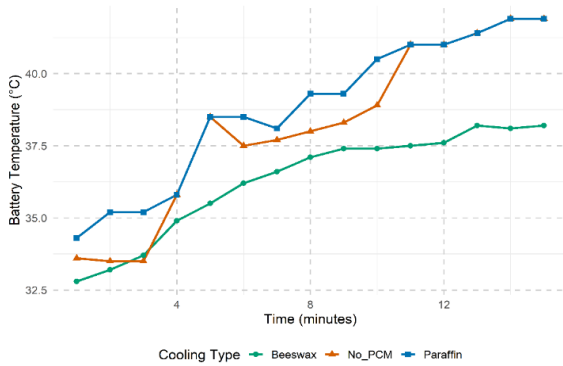

Figure 4. Different battery temperatures against battery with no phase change material (PCM) and with PCM

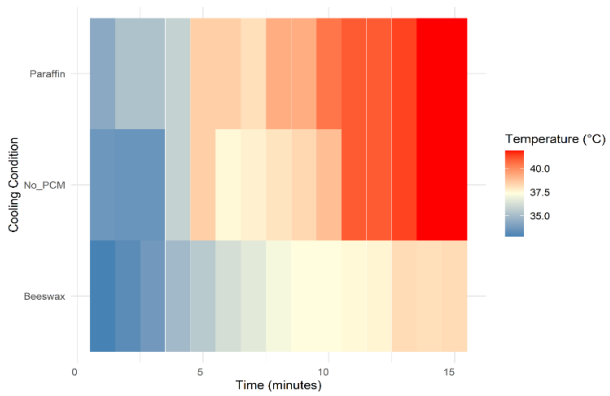

Figure 5. The heatmap of battery temperature under dynamic load

The interaction between load increment and PCM phase transition behavior plays a critical role in temperature divergence among configurations. At lower load levels (0–25%), temperature differences remain minimal because heat generation does not exceed passive dissipation capacity. However, beyond 50% load, heat generation rate increases nonlinearly, amplifying the buffering advantage of PCM materials. This nonlinear interaction explains why temperature gaps widen progressively toward the end of the discharge cycle.

3.2 Electrical stability and voltage behavior

Electrical stability trends in Figure 6 correlate strongly with the observed thermal profiles. The results show that the highest voltage drop occurs in the air-cooled (No PCM) configuration, followed by the paraffin PCM, while the lowest voltage drop is observed in the beeswax PCM configuration. This trend indicates that beeswax PCM not only provides improved thermal regulation but also effectively reduces voltage drop during discharge.

The reduced voltage drop suggests lower internal resistance growth during operation. Since lithium-ion internal resistance increases with temperature, improved cooling performance directly contributes to minimizing resistive losses and stabilizing voltage output [2]. The interaction between thermal buffering and electrochemical behavior explains why even a moderate temperature reduction (≈ 3-4 °C) results in a measurable improvement in voltage stability. In contrast, the air-cooled configuration experiences greater temperature rise, leading to increased resistive losses and consequently higher voltage drop [2].

These findings demonstrate that enhanced thermal management using beeswax PCM contributes not only to temperature control but also to improved electrical efficiency and electrochemical performance of the battery system [2].

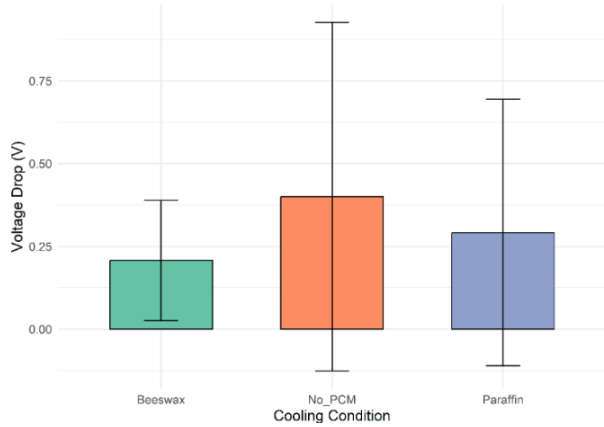

Figure 6. Mean voltage drop (V) under dynamic load conditions for air-cooled (No PCM), paraffin phase change material (PCM), and beeswax PCM configurations

3.3 Mechanical stability of experimental platform

Structural validation using finite element analysis demonstrated that the test rig incurred minimal mechanical stress and displacement (0.1752 MPa and 0.00001101 mm, respectively), indicating that the structure operated well below material yield limits. Ensuring mechanical rigidity is critical in battery thermal experiments to prevent vibration-induced

measurement deviations and structural distortion during dynamic loading conditions, as highlighted in electro-thermal validation studies [28, 29]. The negligible displacement confirms that the physical test platform remained stable and capable of producing reliable thermal measurements. The complete setup is depicted in Figure 7, showcasing the rig's structural design. These mechanical characteristics are further visualized in Figure 8, which presents stress distribution, displacement contours, and safety factor evaluation, consistent with structural validation approaches used in battery system studies [37].

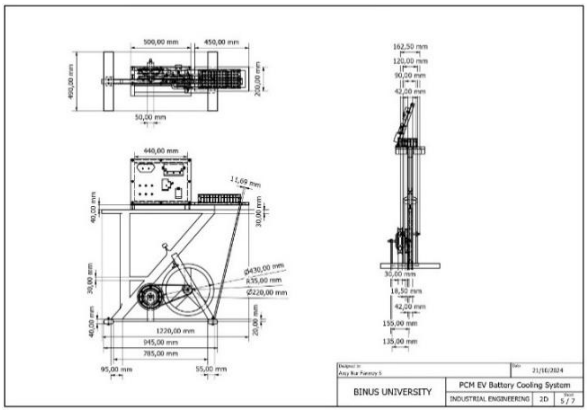

Figure 7. The experimental rig design

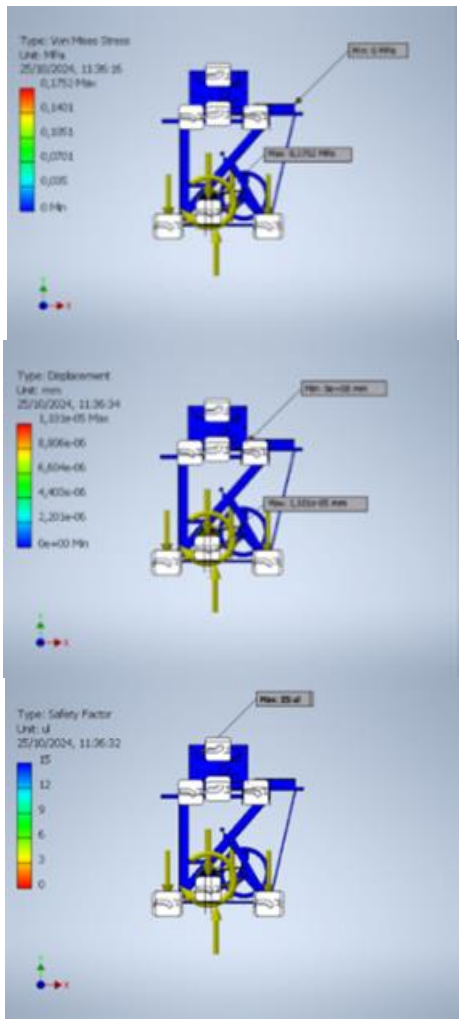

Figure 8. The mechanical characteristics of experimental rig for stress distribution, displacement and safety factor

3.4 Artificial Neural Network predictive modelling and accuracy assessment

The relatively low variance across cross-validation folds (Table 2) indicates that the model generalizes consistently within the tested operating domain. Such stability across folds is consistent with prior studies on ANN-based lithium-ion battery prediction, where controlled network complexity contributes to improved generalization performance [37, 38]. Importantly, the simplicity of the 4–4–1 architecture limit parameter redundancy, thereby reducing overfitting risk given the moderate dataset size.

The close alignment between experimental and predicted temperature (Figures 9 and 10) suggests that the selected input variables, particularly voltage ratio and load level capture, are the dominant contributors to thermal evolution. Similar findings have been reported in neural-network-based electro-thermal estimation frameworks, where load-dependent current variation and resistive heating are identified as primary drivers of temperature dynamics [32]. This indicates that the ANN effectively models the nonlinear coupling between electrical loading and thermal response.

However, prediction accuracy may decrease under stochastic driving profiles or different battery geometries, as model performance is sensitive to variations in operating distribution, a limitation also highlighted in deep-learning-based battery state prediction studies [33]. This reinforces the importance of retraining or fine-tuning the model when extending the framework to different battery configurations or real-world driving scenarios.

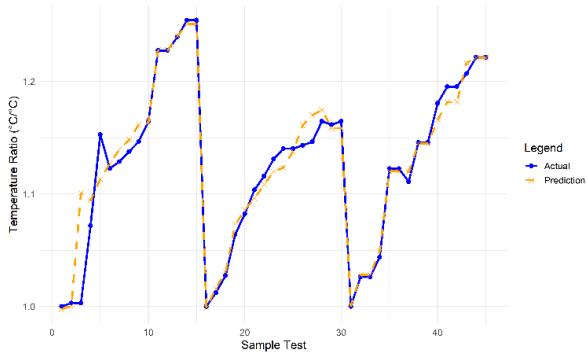

Figure 9. The scatterplot of experimental data and Artificial Neural Network (ANN) simulation data

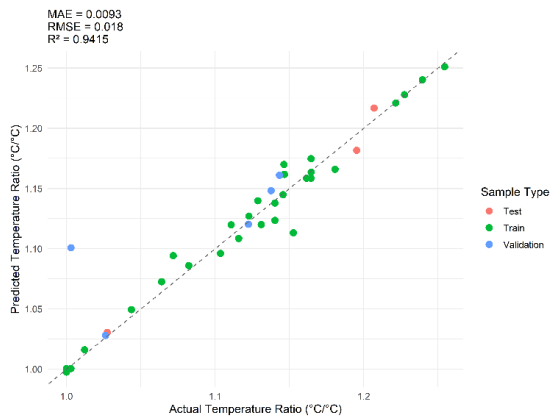

Figure 10. Comparison between experimental battery temperature ratio (°C/°C) and Artificial Neural Network (ANN)-predicted temperature ratio (°C/°C)

The reported R^2 value represents the averaged testing performance across the k-fold cross-validation procedure, confirming that the model was evaluated on unseen subsets and not solely on the training data as shown in Table 2.

Table 2. Performance metrics across 5-fold cross-validation

Fold	MSE	RMSE	MAE	R^2
1	0.00034	0.0184	0.0096	0.936
2	0.00029	0.0170	0.0089	0.948
3	0.00031	0.0176	0.0091	0.943
4	0.00033	0.0181	0.0095	0.938
5	0.00030	0.0173	0.0090	0.946
Average	**0.00031**	**0.0177**	**0.0092**	**0.942**

NOTE: MSE = Mean Squared Error; RMSE = Root Mean Squared Error; MAE = Mean Absolute Error; R^2 = R-squared

The weight values presented in Figure 11 and in the mathematical formulation correspond to the final optimized model obtained after completing the cross-validation training process. Multiple training runs were performed with randomized initialization, and the model exhibiting the lowest averaged validation error was selected as the final representative architecture. Therefore, the reported weight mapping represents the finalized trained model rather than an intermediate or single arbitrary run.

The ANN structure consisted of a 4-4-1 architecture with tanh activation in the hidden layer and linear activation at the output. Weight mapping was clearly defined, supporting transparency and practical applicability in real-time thermal management systems. This is particularly relevant in embedded systems where rapid and accurate temperature forecasting is critical. The architectural design and full weight allocation are presented in Figure 11.

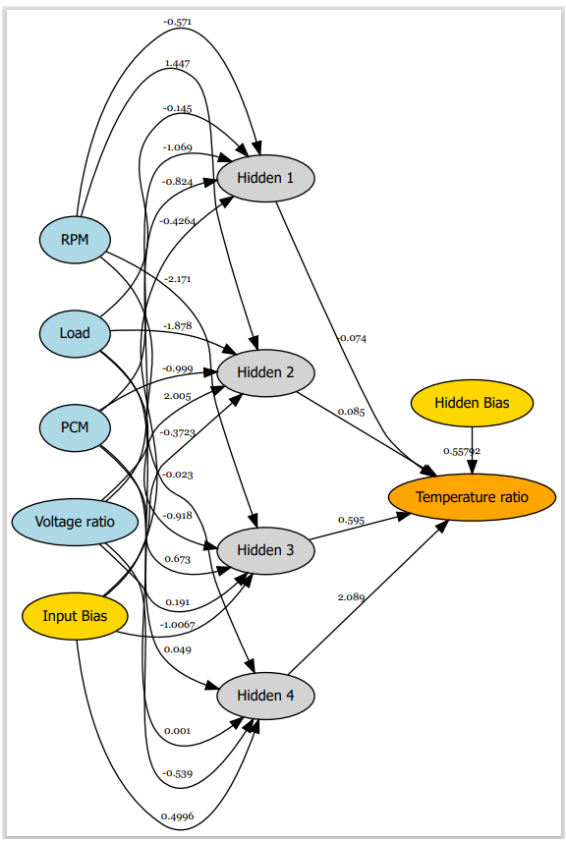

Figure 11. The Artificial Neural Network (ANN) architecture of temperature ratio prediction

The mathematical formulation of the model is as follows:

Let the input vector be X = [*RPM, Load, PCM, Voltage ratio*] with numerical value for *PCM* = 1 for No PCM; 2 for Paraffin; 3 for Beeswax.

Hidden layer computations:

$$h_1 = \tanh(-0.571 \cdot RPM - 0.145 \cdot Load - 1.069 \cdot PCM - 0.824 \cdot Voltage\ ratio - 0.4264) \quad (3)$$

$$h_2 = \tanh(1.447 \cdot RPM - 1.878 \cdot Load - 0.999 \cdot PCM + 2.005 \cdot Voltage\ ratio - 0.3723) \quad (4)$$

$$h_3 = \tanh(-2.171 \cdot RPM - 0.918 \cdot Load + 0.673 \cdot PCM + 0.191 \cdot Voltage\ ratio - 1.0067) \quad (5)$$

$$h_4 = \tanh(-0.023 \cdot RPM + 0.049 \cdot Load + 0.001 \cdot PCM - 0.539 \cdot Voltage\ ratio + 0.4996) \quad (6)$$

Output computation (predicted temperature):

$$y = -0.074 \cdot h_1 + 0.085 \cdot h_2 + 0.595 \cdot h_3 + 2.089 \cdot h_4 + 0.55792 \quad (7)$$

This expression enhances the interpretability and robustness of the ANN approach, facilitating its integration into hybrid battery management frameworks. The study thus validates the synergy between bio-based PCM systems and intelligent predictive modelling, building upon strategies outlined by Dehghani et al. [38].

3.5 Engineering implications for real deployment

While this study primarily focuses on experimental validation and predictive modelling, practical deployment considerations are essential for real-world application. The combined PCM–ANN framework can be integrated into electric scooter battery management systems (BMS) with minimal computational overhead. The selected ANN architecture (4–4–1 multilayer perceptron) is lightweight and suitable for implementation on low-power microcontrollers commonly used in embedded battery management platforms.

In practical deployment, the ANN model could operate in real-time using existing BMS inputs such as pack voltage, current, and temperature. The PCM provides passive thermal buffering, while the ANN functions as a predictive monitoring layer capable of forecasting temperature rise under upcoming load conditions. This predictive capability enables early intervention strategies such as power limitation, current throttling, or rider alert notifications before critical temperature thresholds are reached.

Furthermore, the macro-encapsulated PCM configuration demonstrated in this study is compatible with compact electric scooter battery enclosures without requiring active cooling components. This makes the approach particularly suitable for lightweight micromobility vehicles where space, cost, and energy efficiency are critical constraints.

For broader industrial implementation, future development may include retraining the ANN model using extended driving cycles and multi-environment datasets, enabling adaptive thermal management across different climates and battery

capacities. The proposed framework thus serves as a scalable foundation for intelligent, hybrid passive–predictive battery thermal management systems.

The combined passive–predictive approach demonstrated in this study suggests a scalable architecture for micromobility battery systems. PCM provides passive peak suppression, while ANN prediction enables anticipatory control. In real deployment, the predictive layer could trigger adaptive current limiting before reaching thermal thresholds, thereby reducing degradation risk without requiring bulky active cooling systems.

This hybrid framework shifts battery thermal management from reactive cooling to predictive thermal governance.

4. CONCLUSIONS

This study experimentally and computationally demonstrates that beeswax-based phase change material (PCM) provides superior thermal regulation and electrical stability for lithium-ion batteries in electric scooter applications compared to paraffin PCM and air-cooling systems. The validated experimental rig successfully replicated dynamic operating conditions, while the ANN model accurately predicted battery temperature with high reliability ($R^2 = 0.9415$), confirming its capability to capture non-linear thermal behavior. Despite these promising results, this work is limited to a single battery configuration, a fixed ambient laboratory condition, and short-duration discharge cycles, which may not fully represent long-term aging effects or extreme environmental scenarios. In addition, the intrinsic low thermal conductivity of beeswax and the use of a relatively small experimental dataset may constrain thermal responsiveness and ANN generalization under high-rate or prolonged operation.

From an engineering standpoint, the integration of passive thermal buffering with lightweight predictive modelling provides a feasible pathway toward intelligent battery management in compact electric vehicles. The simplicity of the ANN structure supports embedded deployment without excessive computational demand.

Future research should focus on enhancing beeswax-based PCM through composite or conductive additives, extending experimental validation to diverse ambient conditions and longer cycling durations, and integrating advanced machine learning models with larger datasets for real-time adaptive thermal control. These developments would further strengthen the scalability and practical implementation of intelligent thermal management systems for micromobility and compact electric vehicle applications.

AUTHOR CONTRIBUTIONS

Safarudin Gazali Herawan: Writing – concepts – draft & review. Ismail Azizi Martalogawa, Azqy Nur Farenzy Saputra, Ahmad Hanif: Original draft – data collection – writing.

CONFLICT OF INTEREST

The authors declare that they have no known competing financial interests or personal relationships that could have appeared to influence the work reported in this paper.

DATA AVAILABILITY

The data that support the findings of this study are openly available in Zenodo at https://zenodo.org/records/16686738.

REFERENCES

[1] Sundin, D.W., Sponholtz, S. (2020). Thermal management of Li-ion batteries with single-phase liquid immersion cooling. IEEE Open Journal of Vehicular Technology, 1: 82-92. https://doi.org/10.1109/OJVT.2020.2972541

[2] Mao, G., Jiang, J. (2024). Preparation and application of composite phase change materials. Advances in Computer and Engineering Technology Research, 1(2): 558-563. https://doi.org/10.61935/acetr.2.1.2024.P558

[3] Herawan, S.G., Hanif, A., Martalogawa, I.A., Saputra, A.N.F., Zuraida, R., Ngarianto H., Akop, M.Z.B., Tokit, E.B.M., Sa'at, F.A.Z.B.M., Zakaria, M.S.B., Putra, N.S. D. (2025). The effect of phase change material (PCM) of paraffin and beeswax in battery pack cooling system. IOP Conference Series: Earth and Environmental Science, 1488(1): 012031. https://doi.org/10.1088/1755-1315/1488/1/012031

[4] Talluri, T., Kim, T.H., Shin, K.J. (2020). Analysis of a battery pack with a phase change material for the extreme temperature conditions of an electrical vehicle. Energies, 13(3): 507. https://doi.org/10.3390/en13030507

[5] Madani, S.S., Schaltz, E., Kær, S.K. (2020). Thermal simulation of phase change material for cooling of a Lithium-Ion battery pack. Electrochem, 1(4): 439-449. https://doi.org/10.3390/electrochem1040029

[6] Cattani, L., Malavasi, M., Bozzoli, F., Sciancalepore, C. (2024). Two-phase cooling system for electric vehicles' battery. IOP Conference Series: Journal of Physics, 2766(1): 012011. https://doi.org/10.1088/1742-6596/2766/1/012011

[7] Wen, T. (2025). Advances and challenges in the battery thermal management systems of electric vehicles. Materials, 18(20): 4718. https://doi.org/10.3390/ma18204718

[8] Rahman, M.A., Reddy, G.M., Chatterjee, R., Hait, S., Hasnain, S.M.M., Paramasivam, P., Dabelo, L.H. (2025). Energy sources and thermal management technologies for electric vehicle batteries: A technical review. Global Challenges, 9(7): e00083. https://doi.org/10.1002/gch2.202500083

[9] Behi, H., Karimi, D., Youssef, R., Patil, M.S., Mierlo, J.V., Berecibar, M. (2021). Comprehensive passive thermal management systems for electric vehicles. Energies, 14(13): 3881. https://doi.org/10.3390/en14133881

[10] Yang, Y., Li, W., Xu, X., Tong, G. (2020). Heat dissipation analysis of different flow path for parallel liquid cooling battery thermal management system. International Journal of Energy Research, 44(7): 5165-5176. https://doi.org/10.1002/er.5089

[11] Huo, Z., Hong, X., Li, Y., Chen, Z., Ruan, D. (2024). Numerical study of paraffin and glass fiber composites for thermal management of lithium-ion battery packs. Asia-Pacific Journal of Chemical Engineering, 19(1): e2989. https://doi.org/10.1002/apj.2989

[12] Polat, F., Sarıdemir, S. (2023). Experimental

investigation of the effects of paraffin as a phase change material on the cooling performance of a battery thermal management system. Düzce Üniversitesi Bilim Ve Teknoloji Dergisi, 11(5): 2409-2418. https://doi.org/10.29130/dubited.1379834

[13] Zhao, Y., Jin, L., Zou, B., Qiao, G., Zhang, T., Cong, L., Jiang, F., Li, C., Huang, Y., Ding, Y. (2020). Expanded graphite – paraffin composite phase change materials: effect of particle size on the composite structure and properties. Applied Thermal Engineering, 171: 115015. https://doi.org/10.1016/j.applthermaleng.2020.115015

[14] Liu, C., Xu, D., Weng, J., Zhou, S., Li, W., Wan, Y., Jiang, S., Zhou, D., Wang, J., Huang, Q. (2020). Phase change materials application in battery thermal management system: A review. Materials, 13(20): 4622. https://doi.org/10.3390/ma13204622

[15] Fang, M., Zhou, J., Fei, H., Yang, K., He, R. (2022). Porous-material-based composite phase change materials for a lithium-ion battery thermal management system. Energy & Fuels, 36(8): 4153-4173. https://doi.org/10.1021/acs.energyfuels.1c04444

[16] Bandela, R., Shaik, F. (2025). Modeling of phase change materials in electric vehicle battery thermal management. IOP Conference Series: Materials Science and Engineering, 1334(1): 012007. https://doi.org/10.1088/1757-899X/1334/1/012007

[17] Arumugam, A.B., Buonomo, B., D'Arienzo, C., Romano, P., Manca, O. (2023). A numerical study on thermal control of batteries by phase change materials with liquid cooling. IOP Conference Series: Journal of Physics, 2648(1): 012043. https://doi.org/10.1088/1742-6596/2648/1/012043

[18] Rabiei, M., Gharehghani, A., Saeedipour, S., Andwari, A.M., Könnö, J. (2023). Proposing a hybrid BTMS using a novel structure of a microchannel cold plate and PCM. Energies, 16(17): 6238. https://doi.org/10.3390/en16176238

[19] Dandotiya, D., Joshi, A.K., Kakati, P., Sudharshan, J. (2023). Incorporating copper and carbon nanotube nanoparticles into phase change materials for enhanced thermal management in batteries. Journal of Mines Metals & Fuels, 71(10): 1799-1808. https://doi.org/10.18311/jmmf/2023/35045

[20] Alam, M.S., Das, J.K., Bhowmik, S. (2025). Thermal performance analysis of copper foam enhanced beeswax composite with varying porosity as phase change material for thermal management of Li-ion battery. Physica Scripta, 100(8): 085967. https://doi.org/10.1088/1402-4896/adf6eb

[21] Wang, C.Y., Leong, J.C. (2024). Analysis of thermal management strategies for 21700 lithium-ion batteries incorporating phase change materials and porous copper foam with different battery orientations. Energies, 17(7): 1553. https://doi.org/10.3390/en17071553

[22] Bashirpour-Bonab, H. (2020). Thermal behavior of lithium batteries used in electric vehicles using phase change materials. International Journal of Energy Research, 44(15): 12583-12591. https://doi.org/10.1002/er.5425

[23] Pradeep, R., Venugopal, T. (2021). Investigations on melting and solidification of a battery cooling system using different phase change materials. Thermal Science, 25(4 Part A): 2767-2780. https://doi.org/10.2298/TSCI200229220P

[24] Azzini, F. (2025). Numerical analysis of innovative systems for thermal management of Li-ion batteries using phase change materials. Defect and Diffusion Forum, 445: 267-278. https://doi.org/10.4028/p-F9gewr

[25] Zeng, X., Men, Z., Deng, F., Chen, C. (2022). Optimization of the heat dissipation performance of a lithium-ion battery thermal management system with CPCM/liquid cooling. Materials, 15(11): 3835. https://doi.org/10.3390/ma15113835

[26] Xiao, J., Zhang, X., Bénard, P., Yang, T., Zeng, J., Long, X. (2023). Fin structure and liquid cooling to enhance heat transfer of composite phase change materials in battery thermal management system. Energy Storage, 5(6): e453. https://doi.org/10.1002/est2.453

[27] Jilte, R., Afzal, A., Islam, M.T., Manokar, A.M. (2021). Hybrid cooling of cylindrical battery with liquid channels in phase change material. International Journal of Energy Research, 45(7): 11065-11083. https://doi.org/10.1002/er.6590

[28] Karimi, D., Behi, H., Akbarzadeh, M., Mierlo, J.V., Berecibar, M. (2021). Holistic 1D electro-thermal model coupled to 3D thermal model for hybrid passive cooling system analysis in electric vehicles. Energies, 14(18): 5924. https://doi.org/10.3390/en14185924

[29] Thakur, S.S., Kumar, L. (2024). Numerical study on hybrid battery thermal management system integrating water, phase change material, and fins, under New European Driving Cycle. IOP Conference Series: Journal of Physics, 2766(1): 012221. https://doi.org/10.1088/1742-6596/2766/1/012221

[30] Madani, S.S., Ziebert, C., Marzband, M. (2023). Thermal behavior modeling of lithium-ion batteries: A comprehensive review. Symmetry, 15(8): 1597. https://doi.org/10.3390/sym15081597

[31] Li, S., Cheng, Y., Shen, Q., Wang, C., Peng, C., Yang, G. (2024). Numerical analysis on the thermal management of phase change material with fins for lithium-Ion batteries. International Journal of Numerical Methods for Heat & Fluid Flow, 34(3): 1170-1188. https://doi.org/10.1108/HFF-08-2023-0482

[32] Wang, S., Ren, P., Takyi-Aninakwa, P., Jin, S., Fernandez, C. (2022). A critical review of improved deep convolutional neural network for multi-timescale state prediction of lithium-ion batteries. Energies, 15(14): 5053. https://doi.org/10.3390/en15145053

[33] Chen, S., Zhang, G., Qiao, D., Wang, X., Jiang, B., Dai, H., Zhu, J., Wei, X. (2022). A neural network-based regression study for a hybrid battery thermal management system under fast charging. Sae International Journal of Electrified Vehicles, 11(2): 189-202. https://doi.org/10.4271/14-11-02-0015

[34] Chen, K., Luo, Y., Long, Z., Li, Y., Liu, K., Gao, G., Wu, G. (2025). Robust estimation of lithium-ion battery state of health based on electro-thermal features and machine learning. Proceedings of the Institution of Mechanical Engineers, Part A: Journal of Power and Energy, 239(1): 186-198. https://doi.org/10.1177/09576509241299000

[35] Xie, L., Zhou, H., Gao, M., Yu, H., Mao, B., Zeng, D. (2024). Simulation of health assessment model for thermal management system of lithium-ion battery based on fuzzy clustering algorithm. IOP Conference Series: Journal of Physics, 2771(1): 012011. https://doi.org/10.1088/1742-6596/2771/1/012011

[36] Gao, D., Liu, X., Zhu, Z., Yang, Q. (2023). A hybrid

CNN-BiLSTM approach for remaining useful life prediction of EVs lithium-ion battery. Measurement and Control, 56(1-2): 371-383. https://doi.org/10.1177/00202940221103622

[37] Dong, Y., Ma, X., Wang, C., Xu, Y. (2024). Research on experimental and simulated temperature control performance of power batteries based on composite phase change materials. World Electric Vehicle Journal, 15(7): 302. https://doi.org/10.3390/wevj15070302

[38] Dehghani, F., Eslamloueyan, R., Sarshar, M. (2022). A hybrid model for simulation of lithium-ion batteries using artificial neural networks and computational fluid dynamics. Scientia Iranica, 29(6): 3208-3217. https://doi.org/10.24200/sci.2022.59292.6160

[39] Cao, R., Zhang, X., Yang, H. (2023). Prediction of the heat generation rate of lithium-ion batteries based on three machine learning algorithms. Batteries, 9(3): 165. https://doi.org/10.3390/batteries9030165